The charge-transfer problem in the cluster imitation of ionic crystals with partial covalency

1992 J. Phys.: Condens. Matter 4 5977

(http://iopscience.iop.org/0953-8984/4/27/015)

J. Phys.: Condens. Matter 4 (1992) 5977–5988. Printed in the UK

The charge-transfer problem in the cluster imitation of ionic crystals with partial covalency

He Xiaoguang†§, Huang Meichun†‡ and Lin Hong†

† Department of Physics, Xiamen University, Xiamen, People's Republic of China
‡ Centre of Theoretical Physics, CCAST (World Laboratory), Beijing, People's Republic of China

Received 8 July 1991, in final form 31 December 1991

Abstract. The boundary problems of the widely used cluster method for crystal computations have been investigated, and problems in the cluster calculations of partial ionic crystals were attributed to the charge-transfer problem. The proposed solution, the charge-transfer method, applied to ZnSe and ZnS systems, obtained results comparable to the band-structure calculations for the distributions of the density of states, the energy gaps and the bonding strengths even for the smallest cluster and showed small size effects, which overcame one of the largest deficiencies of the cluster methods. The influences of the charge transfer on the distributions of the density of states were also discussed. The results indicated that the charge-transfer problem is an important factor that should be considered in the cluster imitation of partial ionic crystals.

1. *Introduction*

In the past decade, the cluster method has been widely used to calculate the localized structure in a crystal. It has shown some success, such as a substitutional transition metal (TM) in semiconductors (Hemstreet 1977, 1980, Hemstreet and Dimmock 1979, Fazzio and Leite 1980). In contrast to the Green function technique (Baraff and Schluter 1979), the cluster calculation is simpler and more efficient. It is powerful for strongly localized states such as 3d TM impurities, which need an enormous amount of computation in the Green function method (Zunger and Lindefelt 1983).

However, the existing cluster approaches have a number of distinct drawbacks (Pantelides 1986): (i) convergence of results with cluster size is usually poor (size effect), so that the results are sensitive to the cluster boundary conditions; (ii) it is difficult to determine the precise energy positions of bound states in the gap since the latter, being a bulk property, is not described well by a small cluster; and (iii) it is difficult to get an adequate description of changes occurring in the band continua (resonances and anti-resonances) since the continua are replaced by a set of discrete levels. These drawbacks stem from the disruption of wavefunctions at the cluster boundary, which causes two problems: the dangling-bond problem and the charge-transfer problem.

§ Present address: Department of Electrical Engineering and Computer Science, Northwestern University, Evanston, IL 60208, USA.

0953-8984/92/275977+12$04.50

There have been two methods proposed to eliminate the dangling-bond effect; one is the hydrogen-terminated method. This method has often been adopted for covalent semiconductors such as Si (Hemstreet 1977, 1980, Hemstreet and Dimmock 1979, DeLeo *et al* 1981, 1982a,b), but it is not certain whether this method is applicable to II–VI or III–V semiconductors. Even in the system of Si to which this method is most successfully applied, ambiguity exists in choosing the distance between Si and H, and this influences significantly the convergence of numerical calculations of the energy levels (DeLeo *et al* 1982a). The other method is the sp^3-terminated method proposed by Gemma (1984) for II–VI and III–V semiconductors. This method has the demerit of the insufficiency of orthogonality conditions (Watanabe and Kamimura 1987). But by using strongly localized atomic basis functions, this effect is negligible.

The charge-transfer problem, which is implicit in the normalization property of the formalism in the cluster method, is not solved yet. However, it has a large influence, and sometimes even leads to unreasonable results for a non-neutral cluster (Guo and Ellis 1985, Watanabe and Kamimura 1987, He and Huang 1989). The size effect on the gap and the wrong distributions of the density of states (DOS) are attributed to this deficiency. In addition in this problem, there is the problem of imitating the Madelung potential created by the crystal environment, which is called the environmental potential in this paper.

Tsukada (1980) proposed a method to attack the environmental potential problem. His method partly cancelled the charge accumulation at the boundary, but the charge distribution near the boundary is distorted.

A method of solving the charge-transfer and environmental potential problems simultaneously is proposed in this paper. It will be presented as follows. In section 2, the discrete variational method combined with the self-consistent charge (DVM-SCC) cluster method is reviewed and the origins of the boundary problems are analysed. Then, the solution to the charge-transfer problem, the charge-transfer method, is suggested in section 3 and applied to ZnSe and ZnS systems in section 5. The results are discussed from the points of view of the chemical trend, the size effect, the charge transfer and the impurity calculation. The calculation conditions and the definitions of various clusters are given in section 4. Conclusions are obtained in section 6.

2. Discrete variational method/self-consistent charge cluster method and the origin of boundary problems

The discrete variational method (DVM) (Ellis and Painter 1970) combined with the self-consistent charge (SCC) method (Zunger and Freeman 1977) greatly simplifies the application of the linear combination of atomic orbitals (LCAO) method and saves a lot of computer time. The suggested method is implemented on the basis of the above two approximations.

2.1. DVM-SCC cluster method

In the LCAO method, the wavefunctions of the cluster or molecular orbitals are a linear combination of a set of atomic orbitals. The atomic orbitals $\varphi^s_{nlm}(r)$ are obtained by solving the atomic local density functional (LDF) equation in this paper (Hohenberg and Kohn 1964, Kohn and Sham 1965):

$$\left(-\frac{\nabla^2}{2} - \frac{Z_s}{r} + \int \frac{\rho_s(r')}{|r-r'|}\,\mathrm{d}r' + V_{\mathrm{xc}}[\rho_s(r)]\right)\varphi^s_{nlm}(r) = E^s_{nlm}\varphi^s_{nlm}(r) \qquad (2.1)$$

where Z_s denotes the nuclear charge. In (2.1), $V_{xc}[\rho_s(r)]$ is the exchange–correlation potential. The charge density $\rho_s(r)$ is defined by

$$\rho_s(r) = \sum_{\text{occ}} f^s_{nlm} \varphi^{s*}_{nlm}(r) \varphi^s_{nlm}(r) \tag{2.2}$$

where f^s_{nlm} is the occupation number of nlm atomic orbital.

To exploit the symmetry properties of the cluster, nlm atomic orbitals of pth-shell atoms are combined as the symmetrized bth Γ irreducible representation basis function $\Phi^\Gamma_{pnlb}(r)$:

$$\Phi^\Gamma_{pnlb}(r) = \sum_{s,m} a^\Gamma_{bp,snlm} \varphi^s_{nlm}(r - R_s) \tag{2.3}$$

where the sum over s is taken over the atoms of the pth shell.

Molecular orbital Ψ^Γ_i is expressed as the linear combination of the symmetrized basis functions $\Phi^\Gamma_{pnlb}(r)$:

$$\Psi^\Gamma_i(r) = \sum_{p,n,l,b} C^\Gamma_{i,pnlb} \Phi^\Gamma_{pnlb}(r) \tag{2.4}$$

and governed by the LDF equation in the cluster:

$$H(r) = -\frac{\nabla^2}{2} - \sum_m \frac{Z_m}{|r - R_m|} + \int \frac{\rho(r')}{|r - r'|} \, dr' + V_{xc}[\rho(r)] + V_{\text{out}}(r) \tag{2.5}$$

with $H(r)\Psi^\Gamma_i(r) = E^\Gamma_i \Psi^\Gamma_i(r)$. Here Z_{m} denotes the nuclear charge of the atom in the cluster at the site R_m; $V_{\text{out}}(r)$ is the environmental potential created by the ions outside the cluster. The charge density in the cluster is

$$\rho(r) = \sum_{\Gamma i} f^\Gamma_i \Psi^{*\Gamma}_i(r) \Psi^\Gamma_i(r) \tag{2.6}$$

where f^Γ_i is the occupation number of Γi molecular orbital.

Variation over the combination coefficients in equation (2.4) results in the following linear secular equation:

$$\sum_{pnlb} (H^\Gamma_{p'n'l'b',pnlb} - E^\Gamma_i O^\Gamma_{p'n'l'b',pnlb}) C^\Gamma_{i,pnlb} = 0 \tag{2.7}$$

where $H^\Gamma_{p'n'l'b',pnlb}$ is the Hamiltonian matrix element and $O^\Gamma_{p'n'l'b',pnlb}$ is the overlap matrix element:

$$H^\Gamma_{p'n'l'b',pnlb} = \int \Phi^\Gamma_{pnlb}(r) H(r) \Phi^\Gamma_{p'n'l'b'}(r) \, dr \tag{2.8}$$

$$O^\Gamma_{p'n'l'b',pnlb} = \int \Phi^\Gamma_{pnlb}(r) \Phi^\Gamma_{p'n'l'b'}(r) \, dr. \tag{2.9}$$

With the above formalism, in principle, the self-consistent field calculation can be performed.

The SCC method makes the spherical approximation of the charge density in equation (2.6) to simplify the integration in solving e–e interactions. The charge density ρ has the following form:

$$\rho(r) = \sum_{nls,\Gamma i} f^s_{nl}(\Gamma i) f^\Gamma_i \sum_m \frac{1}{2l+1} |\phi^s_{nlm}(r - R_s)|^2 \tag{2.10}$$

where $f^s_{nl}(\Gamma i)$ is the projected occupation number of the Γi molecular orbital on nl atomic orbital. To realize this approximation, the overlapping charge density among atoms in the cluster is divided among each atomic orbital by the normalized Mulliken population analysis formula:

$$f^s_{nl}(\Gamma i) = \frac{1}{N_p} \sum_{k'pb} \frac{2C^\Gamma_{i,k} C^\Gamma_{i,k'} O^\Gamma_{k,k'}}{C^{\Gamma 2}_{i,k} O^\Gamma_{k,k} + C^{\Gamma 2}_{i,k'} O^\Gamma_{k',k'}} C^{\Gamma 2}_{i,k} O^\Gamma_{k,k} \tag{2.11}$$

where k is short for $pnlb$ and N_p is the number of atoms in the pth shell.

The DVM simplifies the multicentre integrations in equations (2.8) and (2.9) as the summation over a set of pseudo-random integration sampling points $\{r_i\}$ with weight $\{W(r_i)\}$:

$$H^\Gamma_{p'n'l'b',pnlb} = \sum_i W(r_i) \Phi^\Gamma_{pnlb}(r_i) H(r_i) \Phi^\Gamma_{p'n'l'b'}(r_i) \tag{2.12}$$

$$O^\Gamma_{p'n'l'b',pnlb} = \sum_i W(r_i) \Phi^\Gamma_{pnlb}(r_i) \Phi^\Gamma_{p'n'l'b'}(r_i). \tag{2.13}$$

2.2. The origin of the boundary problem

An ideal crystal is an infinite cluster. However, only a finite-size secular equation can be solved or a finite-size cluster, which neglects the interaction between atoms in the cluster and the atoms outside the cluster, can be studied.

For some covalent crystals, the finite cluster approximation gives rise to a serious dangling-bond problem, since the covalent bonds are formed by the sharing of electrons, or the mixing and hybridization of valence orbitals, which form the lower-energy bonding states and higher-energy antibonding states. Dangling bonds usually form electronic states within the band gap where the impurity states of interest are located. Various terminating methods have to be employed.

For the complete ionic crystal, both the dangling bonds and charge transfer are not serious problems, since the ionic bonds are formed by the transfer of electrons. Nevertheless, for the ionic crystal with partial covalency such as II–VI semiconductors, the charge-transfer problem emerges from the calculation method. In the past, the total number of valence electrons required in deciding the occupied states in equation (2.6) is evaluated as if the atoms in the cluster had complete valency, e.g. the Zn^{2+} and S^{2-} in ZnS. However, the absolute value of the real valencies of the atoms in the partial ionic crystal is smaller than the complete valency owing to covalency. The past method results in the overcounting of the net charges for the non-neutral cluster, while the normalization property of the wavefunctions in equation (2.4) and the conservative character of the population analysis formula (2.11) make the extra electrons due to the partial covalency closed in the cluster. Since the total ionicity of the cluster should be completely cancelled by the ionicity of environmental embedding atoms, the ionicity of embedding atoms is also overcounted. This is the so-called charge-transfer problem. It causes an unreasonable distribution of density of states and always results in a larger band gap and distorted effective charges for the atoms in the cluster.

3. The charge-transfer cluster method

Knowing the origin of the boundary problem, we can find a possible way to cure this deficiency. The II–VI semiconductors ZnS and ZnSe will be used as cases to test our method.

Let us first look at the charge distribution in the crystal. ZnS and ZnSe are in the zincblende structure. There are one Zn and one S (or Se) in the unit cell. The net charge of the unit cell is zero, so the effective charge of the cation $(+q)$ should be cancelled completely by the effective charge of the anion $(-q)$. On the other hand, all anions are equivalent and all cations are equivalent; the charge distribution for anions must be the same, so are the cations.

In the cluster method, the atoms of a cluster are chosen according to their distances from a central atom in order to keep the local symmetry of the crystal. The atoms in the cluster form several shells in the order of their distances to the cluster centre. For the zincblende structure, there are one central cation (Zn), four first-shell anions (S or Se), 12 second-shell cations, 12 third-shell anions, six fourth-shell cations, 12 fifth-shell anions and 12 sixth-shell cations, etc. The smallest cluster for this structure is $(Zn_1A_4)^{6-}$, which has -6 net charge. By choosing a different shell, the cluster $(\prod A_{N_i})^{Q_n}$ with different net charge Q_n can be fabricated:

$$Q_n = \sum_i N_i Q_i \tag{3.1}$$

where N_i is the number of atoms in the ith shell and Q_i is the valence charge of the atom in the ith shell, which is $+2$ for Zn and -2 for S and Se in the ideal case. The environmental potentials are obtained by the summation of the Coulomb potential over a large enough point ionic lattice of charge Q_e outside the cluster:

$$V_{\text{out}}(r) = \sum_e \frac{Q_e}{|r - R_e|}. \tag{3.2}$$

The charge-transfer cluster method divides the cluster into inner atoms and boundary atoms $(\prod A_{N_i})_I(\prod A_{N_b})_B$. The method described in section 2 is used to calculate the electronic states of the entire cluster. Upon forming the potential, the charge distributions of the boundary atoms are replaced by the charge distribution of the same species of inner atoms, called the reference atom r. This kind of setting ensures similar charge distributions for the same species of atoms like the situation for them in the crystal. The charge differences between the boundary atoms and the corresponding reference atoms are the charge transfers at the boundary. Since the ground-state properties of the material are uniquely determined by the ground-state charge density, the right charge density should give the right ground-state properties. Now, however, owing to the charge transfer, the net charge of the cluster, Q'_n, becomes

$$Q'_n = \sum_i N_i Q'_i + \sum_b N_b Q'_r \tag{3.3}$$

where N_b is the number of boundary atoms at the bth boundary shell and Q'_r the valence charge of the corresponding reference atom r. The environmental potential must also be adjusted to satisfy the neutral condition of the crystal:

$$V_{\text{out}}(r) = \sum_e \frac{Q_e Q'_n / Q_n}{|r - R_e|}. \tag{3.4}$$

By the above method, the self-consistent calculation of the environmental potential and the transfer of electrons at the cluster boundary can be achieved simultaneously.

Cluster calculations can only give energy levels other than energy bands. Comparison of cluster results with the band structures of the crystal is by total density of states (TDOS) and partial density of states (PDOS), which are yielded in this paper by broadening the levels with a Lorentz profile of broadening coefficient γ and reduce the unit to DOS/(eV unit cell):

$$\text{PDOS} = D^s_{nl}(E) = \sum_{\Gamma i} f^s_{nl}(\Gamma i)\frac{\gamma/\pi}{(E-E_i)^2+\gamma^2} \tag{3.5}$$

$$\text{TDOS} = D_t(E) = \sum_{s,n,l} D^s_{nl}(E). \tag{3.6}$$

4. Calculation models and conditions

The electronic states of five kinds of clusters are calculated by the charge-transfer (CT) cluster method, which will be abbreviated as: cluster A, $(Zn_{1r}Se_{4r})_I(Zn_{12}Se_{12})_B$; cluster B, $(Zn_{1r}S_{4r})_I(Zn_{12}S_{12})_B$; cluster C, $(Zn_1Se_4Zn_{12r}Se_{12r})_I(Zn_6Se_{12})_B$; cluster D, $(Zn_1Se_4Zn_{12r}Se_{12})_I(Zn_6)_B$; and cluster E, $(Mn_1Se_4Zn_{12r}Se_{12})_I(Zn_6)_B$. Here r denotes the reference atoms. Each cluster is embedded in an environmental potential produced by about 1963 point ionic lattices.

Zn(3d,4s), Se(4s,4p), S(3s,3p) and Mn(3d,4s,4p) are treated as valence orbitals and the more tightly bound core orbitals are frozen under the frozen-core approximation. Considering that the charge distributions of boundary atoms are replaced by that of reference atoms inside the cluster, they are not important, and only 4s of Zn, 4p of Se and 3p of S are treated as valence orbitals. To get a better numerical basis, a negative potential well is added when the atomic basis functions are calculated by equation (2.1). The Von Barth and Hedin (1972) formula is adopted to get the exchange–correlation potential in the LDF equations. The broadening coefficient γ in equation (3.5) is 2×10^{-4} Hartree. All figures in this paper are scaled to the Fermi level as the reference zero point, and the peaks in the table are scaled to the highest occupied level.

5. Results and discussion

5.1. The chemical trend

Figure 1 shows the calculated DOS distribution and energy levels for ZnSe (cluster A) and ZnS (cluster B). The shape of the DOS shows very good similarity to the results of experiments (Ley *et al* 1974) and calculations (Zeng and Huang 1988, Wang and Klein 1981). For the sake of comparison with the experiments, the peak notation in Ley *et al*'s (1974) paper will be followed.

For ZnSe, the lowest peak P_{III} is mainly Se:4s (96.2%); then we have the Zn:3d peak, which lies completely below the sp hybridization area beside the energy gap. Within the sp hybridization area of the valence band, three peaks corresponding to peaks P_{II}, S_I and I_I can be recognized clearly. The overall layouts of calculated PDOS agree very well with the band calculation results of the linear muffin-tin orbital

(LMTO) method (Zeng and Huang 1988) and linear combination of Gaussian orbitals (LCGO) method (Wang and Klein 1981). P_{II} are formed by sp hybridization, while S_I and I_I have more Se:4p character.

For ZnS, the distributions of DOS are similar to that of ZnSe. But there are some more weak peaks within the sp hybridization area. These peaks will disappear when a larger broadening coefficient is used. So the results are still qualitatively very good.

Table 1. The calculated peak positions, the energy gaps and sp bandwidths for clusters A and B in comparison with experimental results and calculated results (eV).

	P_{III}	P_{II}	S_I	I_I	d	E_g	W_{sp}
Cluster A	−11.73	−4.60	−1.79	−0.67	−7.39	2.34	5.29
Expt [a]	−13.1	−5.2	−2.6	−1.9	−9.20	2.82	5.6
Expt [a]	−13.7	−4.9	−2.7	−1.3	—	—	—
LMTO[b]	−12.4	−4.72	—	—	−6.34	1.57	5.23
LCGO[c]	−11.83	−4.54	—	—	−6.70	1.83	5.15
Cluster B	−11.65	−4.65	−1.85	−0.73	−7.31	2.80	5.14
Expt [a]	−12.4	−4.9	−3.2	−2.6	−9.03	3.80	5.5
LMTO [b]	−12.1	−4.61	—	—	−6.40	2.49	5.32
LCGO [c]	−11.97	−4.42	—	—	−6.40	2.26	5.20

[a] Ley *et al* (1974).
[b] Zeng and Huang (1988).
[c] Wang and Klein (1981).

Quantitatively, the results are still good. Table 1 lists the calculated results of peak positions, band gaps and sp band widths (W_{sp}) in comparison to the results from experiments and band calculations. For the localized peaks, such as P_{III}, d and lower peak P_{II}, the agreement with the band calculations is very good. The Zn:3d peak is too high compared with the experimental results, which is often considered a deficiency of the LDF formalism rather than the calculation method itself, because there are the same phenomena in the band calculations within LDF. In contrast to

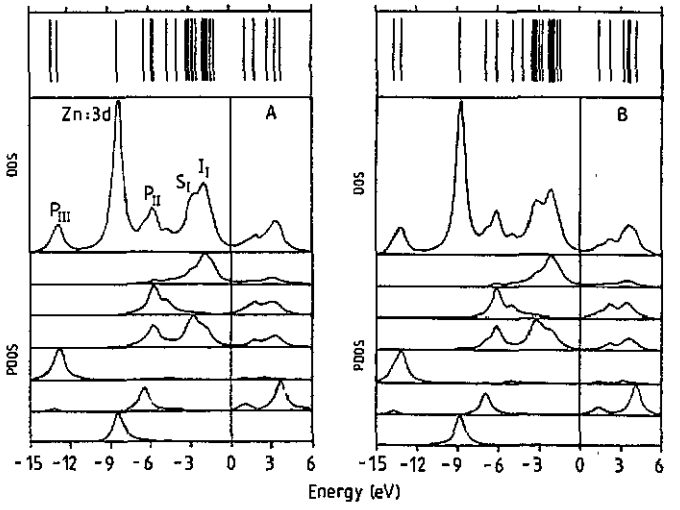

Figure 1. The calculated DOS and PDOS distributions and energy levels for cluster A (ZnSe) and B (ZnS). The PDOS from lower to higher are Zn(centre):3d, Zn(centre):4s, A(1):s, A(1):p, Zn(b):4s and A(b):p. Here A means the anion atom Se or S and b is the boundary atom.

the x-ray photoelectron spectroscopy (XPS) results, the S_I and I_I peaks are too high. One reason is that the energy levels of the cluster calculation are the average of the band structure; the highest occupied level is lower than the exact maximum of the valence band, which is the reference zero point of all peaks below the gap. If about 0.7 eV downward translation of energy is assumed for this factor, all peaks will fit well with experimental results. Similar to the LDF band calculations, the calculated energy gaps, restricted by the precision range of the LDF formalism for the semiconductor calculations, are about 20% smaller than the experimental values. But the calculated gaps are larger than that of the band-structure calculations because the energy levels of the cluster are the average of the band structure. The last parameter listed in table 1 is the width of the sp valence band, which is the mark of covalency of sp bonding. The II–VI semiconductors have stronger ionicity than the III–V and IV semiconductors. But there are still some sp^3 hybridization bonding properties whose strength is measured by the width of the sp valence band. The calculated results agree well with the results from other sources, indicating that the bonding strengths in the CT calculation are appropriate.

The overall chemical trend from ZnS to ZnSe shown in table 1 is right. Although the order of P_{II} peak is not consistent with the chemical trend, the experimental results for the energy difference of this peak between ZnS and ZnSe is only 0.3 eV.

The calculations on ZnSe by the past method show a very poor result compared with the experiment (He and Huang 1989). The Zn:3d levels hybridize with the p levels of Se and sit in the sp band. Even if the charged cluster, which ignores the environmental potential, can get the DOS distribution without the overlapping of Zn:3d levels with the sp band, the peak positions listed in table 2 are very poor compared with experiment. There is the same problem for ZnS (Guo and Ellis 1985). The old method cannot get the right DOS for ZnS and ZnSe.

Table 2. The calculated peak positions and energy gaps by the old method for cluster $(Mn_1Se_4Zn_{12})$, called old A, and charged cluster $(Mn_1Se_4Zn_{12})^{18+}$, called old B (eV).

Cluster	P_{III}	P_{II}	P_I	d	E_g
Old A	−9.73	−0.443	unrecognized	−1.65	3.37
Old B	−9.85	−0.964	unrecognized	−3.83	4.40

5.2. The size effect

The size effect, the crucial deficiency of the cluster method, greatly hindered the application of the cluster method to the calculations of crystals. Watanabe and Kamimura (1987) showed that the gaps are 7.25, 5.91 and 5.60 eV in 17-atom, 41-atom and 59-atom ZnS clusters respectively.

Figure 2 shows the DOS and energy levels of cluster C, which has two more shells of atoms than cluster A. Except for the indistinguishable S_I and I_I peaks, the DOS structures are nearly the same as that of cluster A. The peak positions and band gaps listed in table 2 indicate a very small size effect and are consistent with the corresponding results for cluster A in table 1.

For clusters D and E, which have one shell less boundary atoms than clusters A–C, the DOS structures in figure 3 have the right distribution and not too bad peak positions listed in table 3 in comparison to clusters C and A. But the gaps seem too

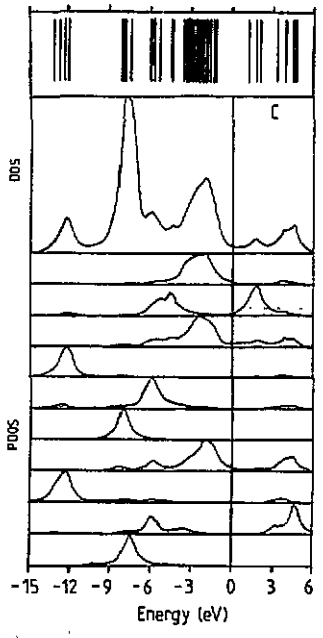

Figure 2. The calculated DOS and PDOS distributions and energy levels for cluster C. The PDOS from lower to higher are Zn(centre):3d, Zn(centre):4s, Se(1):4s, Se(1):4p, Zn(2):3d, Zn(2):4s, Se(3):4s, Se(3):4p, Zn(b):4s and Se(b):4p.

large and the sp band too narrow. We will see in the next part that this is due to too few charges transferred.

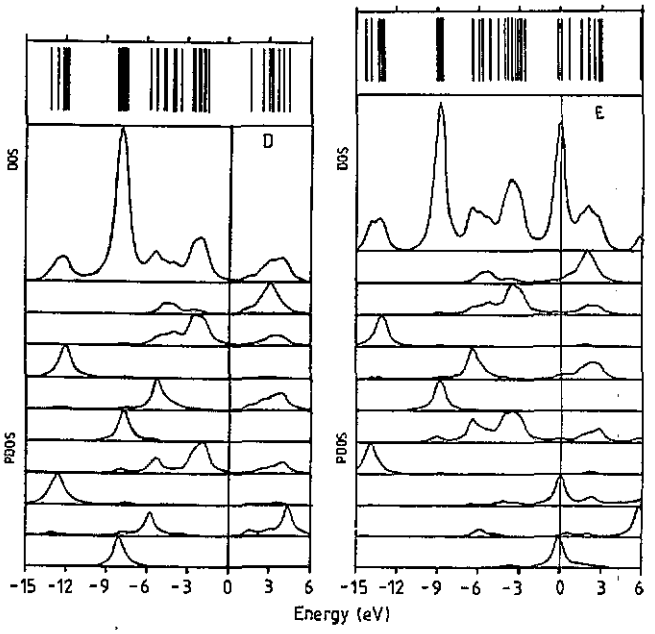

Figure 3. The calculated DOS and PDOS distributions and energy levels for clusters D and E. The PDOS from lower to higher for cluster D are Zn(centre):3d, Zn(centre):4s, Se(1):4s, Se(1):4p, Zn(2):3d, Zn(2):4s, Se(3):4s, Se(3):4p and Zn(b):4s. The PDOS from lower to higher for cluster E are Mn:3d, Mn:4s, Mn:4p, Se(1):4s, Se(1):4p, Zn(2):3d, Zn(2):4s, Se(3):4s, Se(3):4p and Zn(b):4s.

5.3. Charge transfer at the boundary

Compared with the atomic orbital population in table 5 for cluster ($Mn_1Se_4Zn_{12}$),

Table 3. The calculated peak positions, the energy gaps and sp bandwidths for clusters C, D and E. P_i is the average of S_i and I_i (eV).

Cluster	P_{III}	P_{II}	P_I	d	E_g	W_{sp}
Cluster C	−11.14	−4.74	−0.96	−6.53	2.40	4.88
Cluster D	−10.84	−3.84	−0.67	−6.21	3.12	4.28
Cluster E	−10.71	−4.00	−1.43	−6.28	3.23	4.00

Table 4. The atomic orbital population for clusters A, B and E.

	A		B		E			
	Zn	Se(1)	Zn	S(1)	Mn	Se(1)	Zn(2)	Se(3)
Charge s	0.75	1.92	0.80	1.93	0.30	1.93	0.69	1.95
p	—	5.28	—	5.22	0.21	5.21	—	5.32
d	9.99	—	9.99	—	5.35	—	9.99	—
Q_i'	1.26	−1.20	1.21	−1.15	1.14	−1.14	1.32	−1.27
Q_n'	−2.85		−2.73				5.10	
$Q_n' Q_e/Q_n$	0.95		0.91				1.70	

called old A hereafter, and charged cluster $(Mn_1Se_4Zn_{12})^{18+}$, which ignores the environmental potential, called old B hereafter, the effective charges Q_i' of clusters A, B and E in table 4 are very homogeneous. This reaches one of the goals of this work: homogeneous charge distribution of the same species of atoms and the cancellation of the valence charge of anions with that of cations. But the charges transferred at the boundary listed in table 5 for clusters A, B and E are quite different. There are 3.15 and 3.27 charges transferred for clusters A and B, respectively, while there are only 0.9 charges transferred for cluster E. The one boundary shell (12 Se) less in clusters E and D, which accounted for the small charge transfer, drastically increases the band gaps and decreases W_{sp}. The narrower W_{sp} and wider band gaps indicate weaker covalency in just the same way as the band gaps increase from 1.12 eV of Si in IV semiconductors, which is completely covalent crystal, to 3.80 eV of ZnS in II–V semiconductors. The importance of charge transfer at the cluster boundary for the right imitation of partial ionic crystals by a cluster is strongly displayed in this work.

Table 5. The atomic orbital population for clusters old A and old B.

	Old A			Old B		
	Mn	Se(1)	Zn(2)	Mn	Se(1)	Zn(2)
Charge s	0.33	1.95	0.39	0.43	1.95	0.27
p	0.17	4.76	—	0.29	5.02	—
d	5.28	—	9.97	5.32	—	9.99
Q_i	1.22	−0.71	1.63	0.95	−0.97	1.74

It is difficult to say whether the charge transfer or the embedding charge should be blamed for the unreasonable distribution of DOS in the old A cluster. These two factors are inter-entangled. However, considering the fact that the old B has the right

order of peak positions, it seems that a too strong environmental potential due to the ideal embedding charge tends to give an unreasonable DOS distribution. Insufficient charge transfer tends to cause poor peak positions, band gaps and band widths.

5.4. Mn in ZnSe

The DOS and energy levels in figure 3 show that Mn forms highly localized impurity states within the band gap about 2.5 eV above the valence band maximum. The t state is above the e state, which is governed by the T_d symmetry. The composition of the impurity states in table 6 indicates that the e state has more Mn:3d character while the t state has less Mn:3d character due to stronger interaction with host semiconductor states. Numerically, the population numbers on the atomic orbital for cluster E are near that for old B. But $E_t - E_e$ is far smaller than the results from the old method. People usually compare $E_t - E_e$ energy with the crystal splitting energy $10Dq$ in the crystal-field theory, which is 0.54 eV (Langer *et al* 1966). But we do not think there is this equivalence. $10Dq$ in the crystal-field theory is the energy splitting between e and t states under the crystal field with no e–e interaction within d states, while in the mean-field theory all interactions, including the field produced by the electrons in localized states like Mn:3d, are considered. For the localized states, the electronic configurations and occupations have a large influence on the results. For example, in the spin-polarized calculations, the energy difference between t and e states can be twice as large as that from spin-restricted calculations. So the smaller $E_t - E_e$ does not mean a poor result.

Table 6. The population compositions on the impurity orbitals (percentage).

	E		Old A		Old B	
	e	t	e	t	e	t
Mn:3d:	87.3	68.8	85.2	61.2	88.5	68.9
Se:4p	9.1	10.8	14.3	26.2	10.9	17.8
Zn:3s	2.9	9.7	0.4	4.4	0.6	4.0
$E_t - E_e$	0.21		0.46		0.46	

The replacement of Zn by Mn does not have a large effect on the host band. Comparing the DOS of cluster E in figure 3 with that of cluster D in figure 2, which is the replacement of central Mn of cluster E by Zn, we find that Mn:4s has weak hybridization with host atoms but strong charge transfer to the host atoms, which forms the Mn:4s peak in the higher part of the conduction band. The stronger ionicity accounts for the wider band gap and narrower W_{sp}.

6. Conclusions

There are charge-transfer and self-consistent environmental potential problems for the cluster imitation of a partial ionic crystal such as II–VI semiconductors. After the charge-transfer method is suggested to cut off the boundary barrier to charge transfer, results comparable to the band-structure calculations are obtained with a smaller cluster, which is often thought impossible for cluster calculations. The right chemical trend from ZnSe to ZnS, the small size effect, the smaller gaps consistent

with the restriction of LDF formalism and the right distributions of DOS all indicate some success of the charge-transfer method for the ZnSe and ZnS system. Since good results are achieved even with no consideration of the dangling-bond problem in this work, it is argued that charge transfer is the more important factor, which causes the size effect and DOS distribution problem for stronger ionic crystals such as ZnSe and ZnS. The small size effect and right distribution of DOS and PDOS shed light on the solution to the drawbacks of the cluster method. The drawbacks (i) and (ii) in section 1 are problems of the size effect, which is at least not large in the charge-transfer cluster method. Although cluster calculations can only get discrete levels, the right DOS and PDOS distribution combined with the molecular-orbital diagram can facilitate knowledge about the bonding properties even in band continua. In principle, the charge-transfer cluster method can be easily applied to other cluster calculations.

Acknowledgments

This work was performed on the Facom 340 computer at the computing centre of Xiamen University under the support of the National Science Foundation of China (Grant No. 1880736) and the Doctorate Fund of the Education Committee of China (Grant No. 8938401).

References

Baraff G A and Schluter M 1979 *Phys. Rev.* B **19** 4965
DeLeo G G, Watkins G D and Fowler W B 1981 *Phys. Rev.* B **23** 1851
—— 1982a *Phys. Rev.* B **25** 4962
—— 1982b *Phys. Rev.* B **25** 4972
Ellis D E and Painter G S 1970 *Phys. Rev.* B **2** 2887
Fazzio A and Leite J R 1980 *Phys. Rev.* B **21** 4710
Gemma N 1984 *J. Phys. C: Solid State Phys.* **17** 2333
Guo C X and Ellis D E 1985 *J. Lumin.* **33** 345
He X G and Huang M C 1989 *J. Xiamen Univ.* **28** 361
Hemstreet L A 1977 *Phys. Rev.* B **15** 834
—— 1980 *Phys. Rev.* B **22** 4590
Hemstreet L A and Dimmock J O 1979 *Phys. Rev.* B **20** 1527
Hohenberg P and Kohn W 1964 *Phys. Rev.* B **136** 864
Kohn W and Sham L J 1965 *Phys. Rev.* A **140** 1133
Langer D W *et al* 1966 *Phys. Rev.* **146** 554
Ley L *et al* 1974 *Phys. Rev.* B **9** 600
Pantelides S T 1986 *Deep Centers in Semiconductors* ed S T Pantelides (New York: Gordon and Breach) p 7
Tsukada M 1980 *J. Phys. Soc. Japan* **49** 1183
Von Barth U and Hedin L 1972 *J. Phys. C: Solid State Phys.* **5** 1629
Wang C S and Klein B M 1981 *Phys. Rev.* B **24** 3393
Watanabe S and Kamimura H 1987 *J. Phys. Soc. Japan* **56** 1078
Zeng X and Huang M C 1988 *J. Lumin.* **40&41** 913
Zunger A and Freeman J A 1977 *Phys. Rev.* B **15** 4716
Zunger A and Lindefelt U 1983 *Phys. Rev.* B **27** 1191